Lossless Volumetric Medical Image Compression

Youngseop Kim and William A. Pearlman

Center for Digital Video and Media Research
Department of Electrical, Computer, and Systems Engineering
Rensselaer Polytechnic Institute
Troy, New York 12180-3590

ABSTRACT

This paper focuses on lossless medical image compression methods for 3D volumetric medical images that operate on three-dimensional(3D) reversible integer wavelet transforms. We offer an application of the Set Partitioning in Hierarchical Trees (SPIHT) algorithm[1,2] to volumetric medical images, using a 3D wavelet decomposition[3] and a 3D spatial dependence tree. The wavelet decomposition is accomplished with integer wavelet filters implemented with the lifting method, where careful scaling and truncations keep the integer precision small and the transform unitary. We have tested our encoder on volumetric medical images using different integer filters and different coding unit sizes. The coding unit sizes of 16 and 8 slices save considerable memory and coding delay from full sequence coding units used in previous works. Results show that, even with these small coding units, our algorithm with certain filters performs as well and sometimes better in lossless coding than previous coding systems using 3D integer wavelet transforms on volumetric medical images.

Keywords: lossless image compression, volumetric medical image compression, 3D wavelet transfrom, embedded wavelet coding

1. INTRODUCTION

Without efficient compression, the amount of medical data would easily overwhelm the storage and transmission systems. Specially, the problem is more acute for volumetric medical images due to the sheer volume of data. For avoidance of many legal and regulatory issues, lossless compression is desired by doctors for accurate diagnosis and treatment. While intensive attention is paid to a still image compression and video compression, the problem of volumetric image compression is relatively under-investigated.[3]

There exist now several 2D lossless image compression algorithms that are superior to the lossless JPEG standard, such as the Low Complexity Lossless Compression of Images(LOCO-I) algorithm,[4] that is now the new JPEG lossless JPEG standard called JPEG-LS, the Context-based Adaptive Lossless Codec(CALIC) algorithm,[5] and the Compression with Reversible Embedded Wavelets(CREW)[6] . Although they produce good results, such 2D image compression algorithms applied independently to each slice do not exploit inter-slice correlation of volumetric medical images.

In this paper, we report an extension of 2D SPIHT (Set Partitioning in Hierarchical Trees) to 3D that exploits the inter-slice dependence through a 3D wavelet transform and coding along 3D spatial trees. It is the 3D analogue of the progressive lossy to lossless system introduced by Said and Pearlman.[2] Kim and Pearlman[7] have already extended 2D SPIHT to 3D in application to lossy coding of video. The SPIHT algorithm can be stopped at any compressed file-size or let run until nearly lossless reconstruction is obtained, which is desirable in many applications. Bilgin and Marcellin[8] have described a lossless medical image compression scheme that is based on three dimensional(3D) reversible integer wavelet transform and embedded zerotree wavelet (EZW) coding. They have shown it efficiently encodes volumetric data by exploiting the dependencies in all three dimensions, while enabling lossless and lossy compression in the same bitstream. However, as pointed out by Xiong et al.,[9] their lossy results were harmed, because they did not use a unitary transform. In this paper, similar to Xiong et al.,[9] we adopt 3D SPIHT lossless coding of 3D integer wavelet packet transforms of volumetric medical images, but use a much smaller coding unit and hence much smaller memory. Furthermore, we compare compression results obtained with several different integer filter pairs: S+P, I(2,2), I(4,2), and I(2+2,2). Our experiments show that it is possible to obtain comparable and sometimes better compression results with a small coding unit and that I(4,2) appears to be the best choice overall.

The organization of this paper is as follows: Section 2 shows the basic principle of 3D Lossless S+P SPIHT. Integer wavelet packet transform and scaling factor are addressed in section 3. Section 4 provides computer simulation results. Section 5 concludes this paper.

2. SYSTEM OVERVIEW

The proposed volumetric coding system, as shown in Figure 1 and Figure 2, consists primarily of a 3D analysis part, and a coding part with the 3D SPIHT kernel. As we can see, the decoder has the structure symmetric to that of encoder. Slices in a Group of Slice(GOS) will be first axially transformed. Then, each resulting slice will again be separately transformed in the transaxial domain. With our coding system, there is no complication of a rate allocation, nor is there a feedback loop of prediction error signal, which may slow down the efficiency of the system. The axial decomposition in Figure 3 is followed by 2D transaxial decomposition with separable unitary filters.

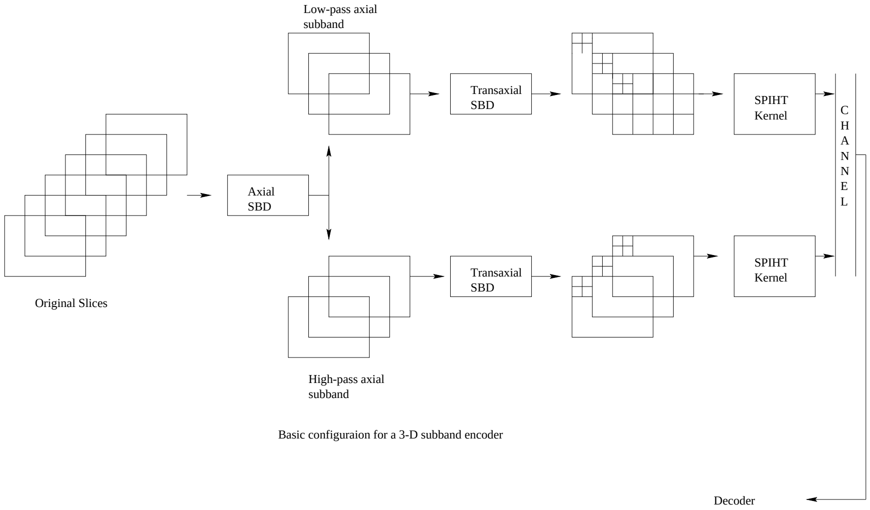

Figure 1. Axial-Tansaxial Subband System Configuration for Encoder

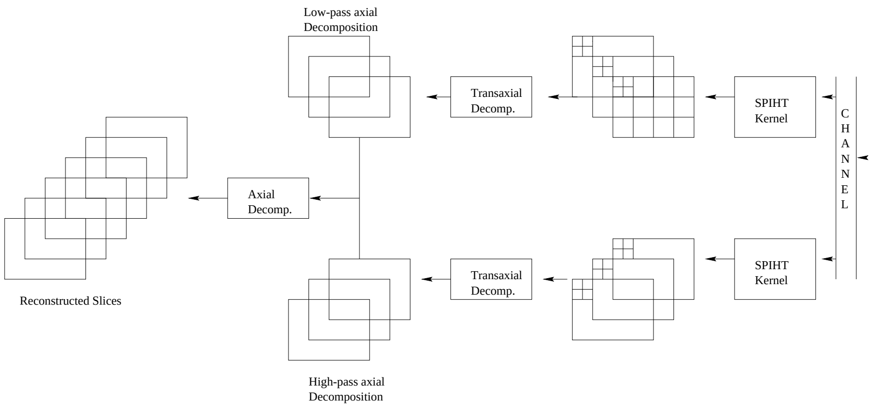

Figure 2. Axial-Transaxial Subband System Configuration for Decoder

Up to now, this axial decomposition is the same as in a previous work.[7] Although the axial high frequency band usually does not contain much energy or correlation, we have found that further dyadic decomposition of this band provides advantages in PSNR (peak signal to noise ratio) and visual quality with SPIHT coding. The similar idea of so called wavelet packet decomposition[10] also produced better visual quality than purely dyadic decomposition of the low frequency bands.

In Figure 5, we show the complete subband structure to two complete levels of decomposition. In this figure, H_t and L_t represent axial-highpass and lowpass subbands respectively, and H_h, L_h, H_v, and L_v represent transaxialhorizontal highpass, lowpass, transaxial-vertical highpass, and lowpass bands respectively. A total of 28 subbands results from the 2-level axial-transaxial wavelet decomposition in Figure 5. An important issue associated with 3D SBC/Wavelet is the choice of filters. Different filters in general show different signal characteristics in the transform domain in terms of energy compaction and high frequency error signal.[11] The recent introduction of wavelet theory offers promise for designing better filters for image/video coding.[11]

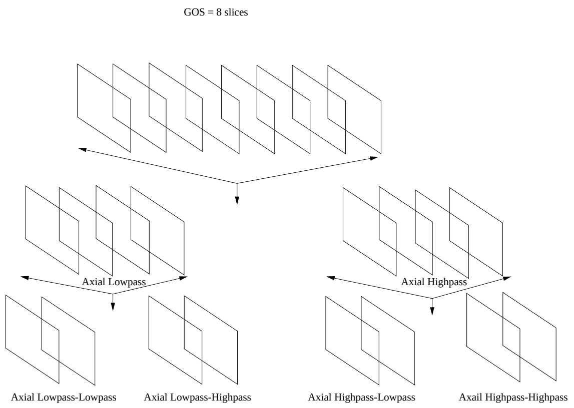

Figure 3. Axial Subband Decomposition

We now define parent-offspring relationships in a tree of wavelet coefficients. For 2D SPIHT[1] the parent-offspring dependencies are shown in Figure 6, where a node consists of 4 pixels, and a tree is defined such that each pixel in a node has either four offspring or no offspring in the case of a leaf node. (The transform coefficients are often called pixels.) In 3D SPIHT,[7] a node forms 8 pixels of 2x2x2 pixels. Each non-leaf pixel has 8 offspring pixels and only one parent pixel if also not a root pixel. Except for root and leaf pixels, all pixels adopt the following formula for parent- offspring relationships in hierarchical tree. Let $\mathcal{O}(i,j,k)$ denote a set of offspring pixels of a parent pixel (i,j,k). Then,

$$\begin{array}{l} \mathcal{O}(\text{i,j,k}) = \{ \\ (2i,2j,2k),\ (2i+1,2j,2k),\ (2i,2j+1,2k), \\ (2i+1,2j+1,2k),\ (2i,2j,2k+1),\ (2i+1,2j,2k+1), \\ (2i,2j+1,2k+1),\ (2i+1,2j+1,2k+1) \\ \}. \end{array} \tag{1}$$

In Figure 7, we depict the 3D parent-offspring dependencies.

3. 3D INTEGER WAVELET PACKET TRANSFORM AND SCALING FACTOR

In this section, we construct wavelet transforms that map integers to integers and show the careful scaling and truncations that keep the integer precision small and the transform unitary.

In this work we denote by $c_{0,j}$ the original signal of interest, $l_{1,j}$ and $h_{1,j}$ the lowpass and highpass coefficients respectively after a wavelet transform. We present constructions of wavelet transforms that make a signal $c_{0,j}$ represented in integers to $l_{1,j}$ and $h_{1,j}$, also represented in integers. The transform is reversible, i.e., we can exactly recover $c_{0,j}$ from $l_{1,j}$ and $h_{1,j}$. We use the S+P integer filter[2] and other integer filters.[11]

The set of transforms has names of the form(N,Ñ), where N is the number of vanishing moments of the analyzing high pass filter, while Ñ is the number of vanishing moments of the synthesizing high pass filter (vanishing moments correspond to the multiplicity of zero as a root in the spectrum of the filter).

I(2,2) filter:

$$\begin{aligned} h_{n,m} &= c_{n-1,2m+1} - \lfloor 1/2(c_{n-1,2m} + c_{n-1,2m+2}) + 1/2 \rfloor \\ l_{n,m} &= c_{n-1,2m} + \lfloor (h_{n,m-1} + h_{n,m})/4 + 1/2 \rfloor \end{aligned} \tag{2}$$

I(4,2) filter pair:

$$\begin{aligned} h_{n,m} &= c_{n-1,2m+1} - \lfloor 9/16(c_{n-1,2m} + c_{n-1,2m+2}) - 1/16(c_{n-1,2m-2} + c_{n-1,2m+4}) + 1/2 \rfloor \\ l_{n,m} &= c_{n-1,2m} + \lfloor (h_{n,m-1} + h_{n,m})/4 + 1/2 \rfloor \end{aligned} \tag{3}$$

I(2+2,2) filter pair:

$$\begin{aligned} h^1_{n,m} &= c_{n-1,2m+1} - \lfloor 1/2(c_{n-1,2m} + c_{n-1,2m+2}) + 1/2 \rfloor \\ l_{n,m} &= c_{n-1,2m} + \lfloor 1/4(h^1_{n,m-1} + h^1_{n,m}) + 1/2 \rfloor \\ h_{n,m} &= h^1_{n,m} - \lfloor 1/8(-1/2 l_{n,m-1} + l_{n,m} - 1/2 l_{n,m+1}) + 1/8(-1/2 l_{n,m} + l_{n,m+1} - 1/2 l_{n,m+2}) + 1/2 \rfloor \end{aligned} \tag{4}$$

S+P filter pair:

$$\begin{aligned} h_{n,m} &= c_{n-1,2m+1} - c_{n-1,2m} \\ l_{n,m} &= c_{n-1,2m} + \lfloor (h_{n,m})/2 \rfloor \\ \hat{h}_{n,m} &= -1/16(h_{n,m}) + \lfloor \alpha(c_{n-1,2m-1} - c_{n-1,2m})) + \beta(c_{n-1,2m} - c_{n-1,2m+1}) + \gamma(h_{n,m+1}) + 1/2 \rfloor \end{aligned} \tag{5}$$

The S+P filters in Equation(5) first form the S transform in the expressions for $h_{n,m}$ and $l_{n,m}$ and then uses an extra prediction step to obtaining the high pass filter coefficient $\hat{h}_{n,m}$. In previous works,[12,8] the predictor parameters $\alpha = 2/8$, $\beta = 3/8$, and $\gamma = 2/8$ were selected, but we select $\alpha = 3/16$, $\beta = 8/16$, and $\gamma = 6/16$ to get better performance for medical images. The I(4,2) filter pair in (3) is inspired by the S+P transform, whereby one extra lifting step in the high pass part of the I(2,2) filter pair in Equation (2) produces a high pass filter with 4 vanishing moments.

The S+P transform produced by the filters in Equation (5) is not unitary, but we would have an approximately unitary transform only for 2D, if, prior to the prediction or lifting, we had used as a basis

$$\begin{aligned} h_{n,m} &= (c_{n-1,2m+1} - c_{n-1,2m})/\sqrt{2} \\ l_{n,m} &= (c_{n-1,2m} + \lfloor (h_{n,m})/2 \rfloor)/\sqrt{2} \end{aligned} \tag{6}$$

instead of the S transform. It is only approximately unitary, due to the downward truncations needed to form the low-pass band. Applying this transform separably in each of two dimensions produces a scaling by 1/2, a factor of perfect integer precision. However, we cannot use the above Equation (6) for 3D, because the scaling factor now becomes a floating point number requiring precision truncation. However, if we choose a decomposition requiring an even number of decompositions for each subband, we can ensure perfect integer precision. This dictum holds true for all the integer transforms, because they are all built from the S transform. In Figure 4, we have shown a decomposition and the implicit scaling of the wavelet transform pyramid to approximate a 2D 2-level unitary integer wavelet transform. The 3D axial-transaxial packet transform in Figure 8 obeys the even decomposition number rule for each subband, so that implicit scaling by powers of two results in a unitary transform of perfect integer precision. However, a unitary transform is required only for lossy coding, not for the lossless coding considered in this work. In the future, we intend to report on the use of this system for lossy coding. Nevertheless, for the sake of completeness, we show in Figure 5 the required implicit scaling factors needed to obtain (approximately) unitary transforms and that were used in our experiments.

4. RESULTS

We used 256 by 256 8-bit images from Mallinckrodt Institute of Radiology Image Processing Laboratory[13] and Group of Slices (GOS) = 16 and 8 slices for $l = 3$ and 2 levels of decomposition, respectively, in both the axial and transaxial domains. This constraint to three levels of decomposition is the most that can be applied to the axial direction, so that limiting the transaxial levels to three may prevent further exploitation of transaxial redundancy for a relatively larger size of volumetric slice.

We shall assess the effect of GOS size on the performance of 3D SPIHT S+P and 3D Integer wavelet filters. In general, a larger size of GOS is expected to give better compression performance. We use two different size GOS's,16 and 8, to test with the same volumetric sequence. In all cases, we perform 3 and 2 levels of transaxial/axial decomposition with the following integer wavelet filters: S+P, I(2,2), I(4,2), and I(2+2,2). Lossless coding rates in bits per pixel for five volumetric images are shown in Table 1. We have used arithmetic coding to encode the significance decision bits in the SPIHT output bitstream to improve our lossless coding performance.

To establish a reference to assess gains of 3D over 2D lossless coding, we have included in Table 1, volume image compression results with two-dimensional (GOS=1) SPIHT/S+P,[12,2] LOCO-I,[4] and CALIC.[5] As you see in Table 1, 2D alogrithms are on the average about 30 to 38% worse than 3D algorithms in compression performance. Bilgin and Marcellin[8] used a 2-level dyadic implementation of the (2,4) and (2+2,2) interpolating integer wavelet transform

Figure 4. Tree structure for 2D integer wavelet transform with 2 levels. Scaling factors for integer filters to obtain unitary transform.

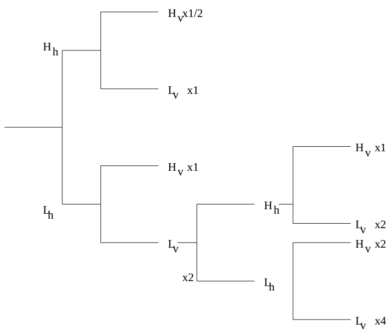

on 16 slice volumes. However, in Table 1, they obtained superior results by a small margin for only the MRhead image and 10% worse results otherwise. Xiong ,Wu, and Yun[9] used a single coding of unit all the slices in the volume, and a 4-level integer wavelet packet transform. Their implementation requires memory on the order of 2-3 times the whole volume image. (All the wavelet coefficients and the sorting lists LIP, LIS, and LIP are required to be in active memory.) Even though Xiong's results are the best for "MRchest" and "CTskull" with the I(2+2,2) filter, they are no more than 2% better than SPIHT with GOS of 16 with the I(2+2,2) or I(4,2) filter. Surprisingly, that 3-level coding unit of 16 slices with I(4,2) integer filter gave slightly better compression than the I(2+2,2) integer filter with four levels of decomposition of the whole image volume by XIONG for the "MRhead image". In fact, the compression performance of both implemetations was almost identical for the I(2+2,2) filter. The GOS of 16 outperforms the smaller size of GOS in all image and I(4,2) wavelet filter outperforms other filters for "MRhead" , "MRlivert1", and "MRlivert2" medical volumetric images. We again see that GOS of 16 outperforms the smaller GOSs.

Method	GOS	Filter	MRchest	MRlivert1	MRlivert2	MRhead	CTskull
3D SPIHT	16	S+P	2.1045	2.3979	1.7883	2.2400	2.1134
3D SPIHT	16	I(2,2)	1.8105	2.3473	1.7713	2.2383	2.1081
3D SPIHT	16	I(4,2)	1.7835	**2.159**	**1.626**	2.2040	2.0464
3D SPIHT	16	I(2+2,2)	1.7790	2.1892	1.7321	2.2355	2.1023
3D SPIHT	8	S+P	2.2000	2.5443	1.9169	2.2460	2.3210
3D SPIHT	8	I(2,2)	1.9988	2.4198	1.7947	2.2500	2.3318
3D SPIHT	8	I(4,2)	1.9134	2.3377	1.7831	2.2430	2.2980
3D SPIHT	8	I(2+2,2)	1.9017	2.3982	1.7923	2.2743	2.3133
2D SPIHT	1	S+P	2.8555	3.1288	2.4982	2.6913	2.6823
2D SPIHT	1	I(4,2)	2.8554	3.1130	2.4329	2.6956	2.6921
LOCO-I[4]	1		2.9282	3.1582	2.3692	2.5567	2.8460
CALIC[5]	1		2.8102	2.5451	2.2432	2.5851	2.7250
3D IEZW[8]	16	I(2,4),I(2+2,2)	2.0225	2.3983	1.7607	**2.1955**	2.2005
XIONG[9]	64,48,192	I(2+2,2)	**1.7680**			2.2320	**1.995**

Table 1. Lossless Coding Results(bit/pixel)

5. CONCLUSIONS

In this paper, we introduced 3D lossless SPIHT medical image compression methods for 3D volumetric medical images that operate on three-dimensional reversible integer wavelet transforms. The result shows that this algorithm performs quite well for 3D lossless medical images. Our 3D lossless SPIHT algorithm produces up to 30–38% decrease in compressed file sizes compared to the best 2D lossless image compression algorithms. Our algorithm performs better than 3D Improved Embedded Zerotree Wavelet (IEZW),[8] which used 2-level dyadic decomposition in each dimension on 16 slice coding units, and a similar 3D SPIHT[9] that used the four levels of decomposition in each

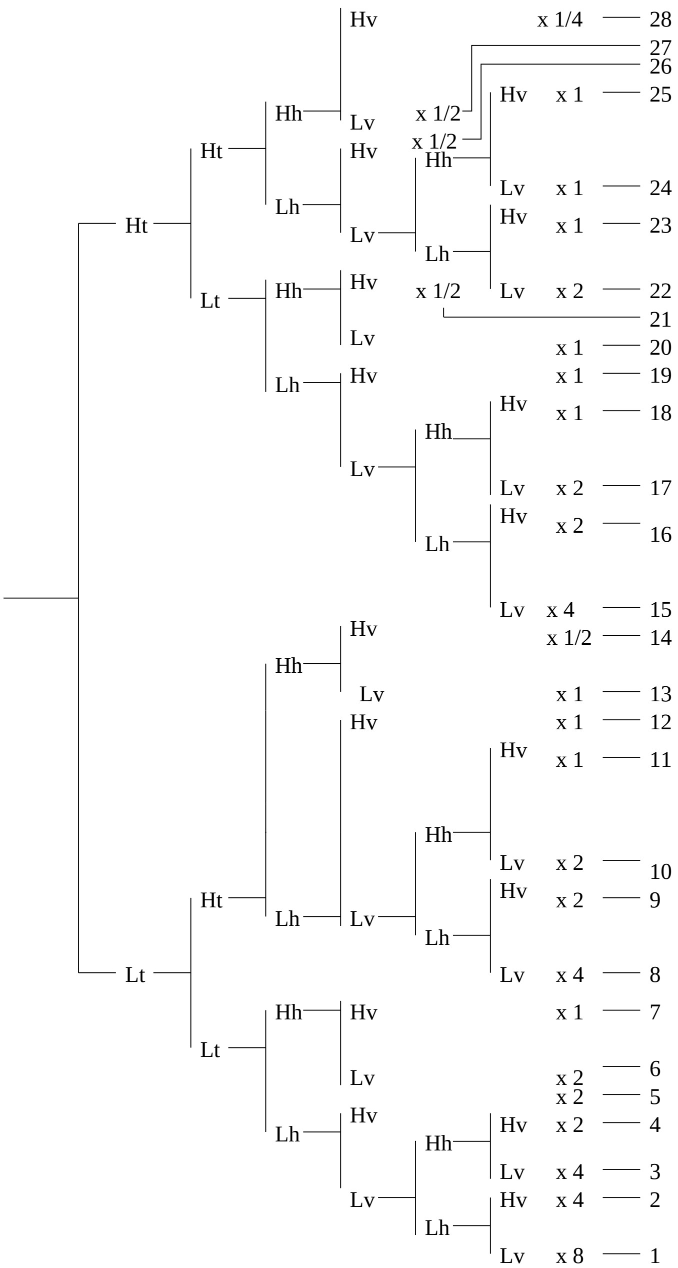

Figure 5. Tree structure for 3D integer wavelet transform with 2 levels. Scaling factors for integer filters to obtain unitary transform.

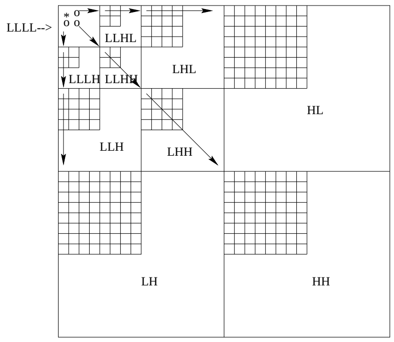

Figure 6. 2D parent-offspring dependencies

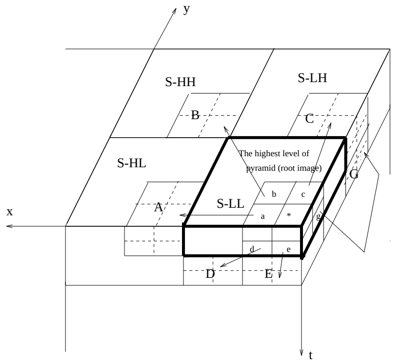

Figure 7. 3D parent-offspring dependencies

dimension for full sequence coding units. A smaller coding unit saves considerably in dynamic memory usage and does not cause noticeable degradation and may even improve performance for proper filter choices.

ACKNOWLEDGEMENT

This work was supported in part by the National Science Foundation under Grant Nos. NCR-9523767 and EEC-9812706. The government has certain rights in this material.

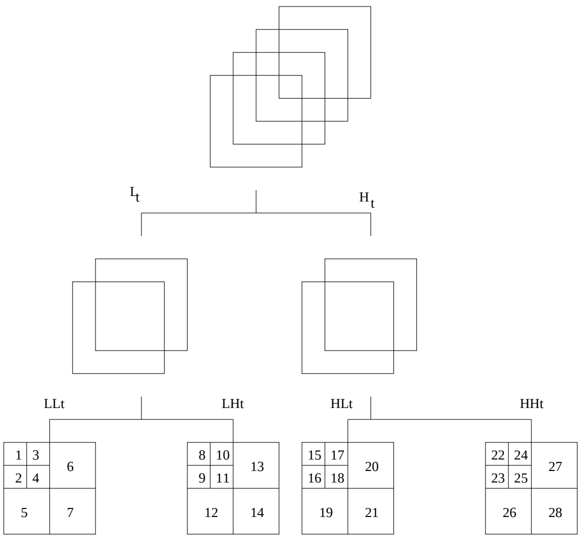

Figure 8. Axial-Transaxial integer wavelet packet transform with 2 levels

REFERENCES

1. A. Said and W. A. Pearlman, "A new, fast and efficient image codec based on set partitioning in hierarchical trees," *IEEE Trans. on Circuits and Systems for Video Technology* **6**, pp. 243–250, June 1996.
2. A. Said and W. A. Peralman, "An image multiresolution representation for lossless and lossy image compression," *IEEE Trans. on Image Processing* **5**, pp. 1303–1310, Sept. 1996.
3. J. Luo, X.Wang, C.W.Chen, and K. J.Parker, "Volumetric medical image compression with three-dimensional wavelet transform and octave zerotree coding," *Proceedings SPIE* **2727**, pp. 579–590, 1996.
4. M.J.Weinberger and G.Sapiro, "$loco-i$: A low complexity, context based lossless image compression algorithm," *Proc. of Data Compression Conference* , pp. 140–149, 1996.
5. X.Wu and N.Menon, "*calic*–a context based adaptive lossless image codec," in *Image Processing*, *Proc. of International Conference on Acoustic, Speech and Signal Processing* **4**, pp. 1890–1893, 1996.
6. A. Zandi, J. D.Allen, E. L.Schwartz, and M. Boliek, *Compression with Reversible Embedded Wavelet*, $RICOH$ California Research Center Report, 1997.
7. B. Kim and W. A. Pearlman, "An embedded wavelet video coder using three-dimensional set partitioning in hierarchical tree," in *Image Processing*, *Proc. of Date Compression Conference* , pp. 252–260, 1997.
8. A. Bilgin and M. W.Marcellin, "Efficient lossless coding of medical image volumes using reversible integer wavelet transforms," in *Image Processing*, *Proc. of Data Compression Conference* , March 1998.
9. Z. Xiong, X. Wu, and D. Y.Yun, "Progressive coding of medical volumetric data using three-dimensional integer wavelet packet transform," in *Image Processing*, *IEEE Workshop on Multimedia Signal Processing* , pp. 553–558, Dec. 1998.
10. Z.Xiong, K.Ramchandran, and M.T.Orchard, "Wavelet packet image coding using space-frequency quantization," *IEEE Trans. on Image Processing* **7**, pp. 892–898, June 1998.
11. M.Vetterli and J.Kovacevic, *Wavelets and Subband Coding*, Prentice Hall, Inc, 1995.
12. A. Said and W. A. Pearlman, "Reversible image compression via multiresolution representation and predictive coding," in *Visual Communications and Image Processing '93*, *Proc. SPIE* **2094**, pp. 664–674, Nov.1993.
13. Mallinckrodt Institute of Radiology Image Processing Laboratory, ftp://carlos.wustl.edu.